의학박사 학위논문

Development of a surrogate marker for P-glycoprotein expression in drug-resistant epilepsy using the (*R*)-[^{11}C]-Verapamil PET/MR with cyclosporine

난치성 뇌전증에서 사이클로스포린과 (*R*)-[^{11}C]-Verapamil PET/MR을 이용한 P-glycoprotein 발현의 대리표지자 개발

2016 년 2 월

서울대학교 대학원

의학과 협동과정 임상약리학과 전공

신 정 원

ABSTRACT

Jung-Won Shin
Clinical pharmacology
The Graduate School
Seoul National University

Background and Purpose: The development of resistance to antiepileptic drugs is explained well by the transporter hypothesis, which suggests that drug resistance is caused by inadequate penetration of drugs into the brain barrier as a result of increased levels of efflux transporter such as p-glycoprotein. To evaluate the brain expression of p-glycoprotein (Pgp) in patients with drug-resistant epilepsy (DRE), including neocortical epilepsy, we developed a non-invasive quantitative analysis including asymmetry indices (AIs) based on (*R*)-[^{11}C]-verapamil PET/MRI with cyclosporine (CS); a Pgp inhibitor.

Materials and Methods: Nine patients with DRE, five patients with drug-sensitive epilepsy (DSE), and eight healthy subjects underwent dynamic (*R*)-[^{11}C]-verapamil PET/MRI with an intravenous infusion of CS. AIs [(right region – left region)/(right region + left region) $\times 200\%$] of the standard uptake values in each of the paired lobes were calculated.

Results: All DRE patients, except for patients with parietal lobe epilepsy, had significantly different asymmetry from the healthy subjects, whereas all DSE patients had asymmetry similar to healthy subjects. In the temporal lobe, the

AIs of patients with left temporal lobe DRE were more positive than those of healthy subjects (healthy subjects: 4.0413 ± 1.7452; patients: 7.2184 ± 1.8237; $p = 0.048$), and those of patients with right temporal DRE were more negative (patients: -1.6496 ± 3.4136; $p = 0.044$). In addition, specific regions which had significant asymmetry were different between lateral and medial temporal lobe epilepsy groups. In the frontal lobe, the AI of patient with right frontal lobe DRE was more negative than healthy subjects.

Conclusions: We confirmed that Statistical Parametric Mapping analysis using AIs of (*R*)-[^{11}C]-verapamil PET/MRI with CS could be used as a surrogate marker for DRE, and this approach might be helpful for localizing or lateralizing the epileptic zone. **ClinicalTrials.gov number:** NCT02144792

Keywords: P-glycoprotein, Drug-resistant epilepsy, Surrogate marker, PET/MR, (*R*)-[^{11}C]-verapamil

Student number: 2012-21775

CONTENTS

LIST OF TABLES AND FIGURES

INTRODUCTION

Epilepsy, which is characterized as recurrent spontaneous seizures, is one of the most common neurological disorders.[1] Despite the development of third-generation antiepileptic drugs (AEDs) over the past three decades, 20–30% of patients with epilepsy remain resistant to drug treatment.[2, 3] The mechanisms of drug resistance in epilepsy remain unclear. Among the mechanisms of drug resistance in epilepsy, increasing experimental and clinical evidence supports the transporter hypothesis.[4] Several studies have suggested that the increased expression of efflux transporters, such as p-glycoprotein (Pgp), at the blood–brain barrier (BBB) in the focal tissue, limits the penetration of AEDs into the focus.[5, 6] In the human brain, Pgp exhibited a highly localized overexpression on the vascular endothelium as well as the end-feet of the vascular glia in cases of drug-resistant epilepsy (DRE).[7]

Consequently, the problem of drug resistance in epilepsy might be resolved by the development of a new treatment strategy targeting the transporter mechanism. To develop such a strategy, surrogate markers should objectively pinpoint the expression of transporters such as Pgp. More importantly, surrogate markers should be used non-invasively to render the technique readily applicable in clinical practice. Several recent clinical trials have evaluated Pgp expression in humans via positron emission tomography (PET) using the Pgp substrate (*R*)-[^{11}C]-verapamil and Pgp inhibitors, such as tariquidar or cyclosporine (CS).[8, 9] Several investigators have performed (*R*)-

[^{11}C]-verapamil PET in epileptic patients to compare the expression of Pgp between DRE patients and healthy subjects, using the (%) changes in verapamil influx or efflux rate before and after Pgp inhibitor injection. However, to our knowledge there has been no study for MR-negative neocortical epilepsies, and previous methods were applied only to medial temporal lobe epilepsy. Furthermore, they confirmed that the change in verapamil influx rate was smaller in DRE patients compared with healthy subjects; this necessitated the use of complex analytical methods, including invasive serial arterial sampling which has limited applicability in clinical practice.

Another problem is that, in (*R*)-[^{11}C]-verapamil PET, it is impossible to find focal hypo- or hyper - radio uptake regions, because when using the Pgp inhibitor, individually distinct Pgp functions of the whole brain and regional differences in Pgp expression may result in interindividual variability of radiotracer uptake in the whole brain and specific brain regions.[10 11]

Therefore, to develop a more feasible surrogate maker that can be used in clinical practice, we performed (*R*)-[^{11}C]-verapamil PET and magnetic resonance imaging (MRI) with intravenous infusion of cyclosporine without serial arterial sampling (VPM-PET/MR-CS). The subject population comprised drug-resistant and seizure-free patients with various types of epilepsy, including MR-negative neocortical epilepsy. We analysed the data using statistical probabilistic anatomical mapping (SPAM) with the asymmetry index (AI) of the standard uptake value (SUV). We hypothesized

that Pgp activity is higher in the epileptic foci compared with that in the contralateral normal area within drug-resistant patients, and the asymmetry will be larger than that in healthy persons or seizure-free patients.

METHODS

1. Subjects

Patients with epilepsy (age range, 18–53 years) who were either drug-resistant or drug-sensitive were recruited between January 2013 and March 2014 from epilepsy clinics at Seoul National University Hospital. All patients had been examined for 24 h using video electroencephalography monitoring (VEM), and patients with DRE had previously undergone pre-surgical evaluation. DRE was defined as the failure of adequate trials of two tolerated and appropriately chosen and used AED schedules (whether as monotherapies or in combination) to achieve sustained freedom from seizures.[12] Seizure-free drug-sensitive epilepsy (DSE) was defined as a well-controlled state, free of all seizures, in a patient receiving AEDs for at least 1 year prior to PET scanning. We investigated the baseline characteristics and the results of the previous VEM, brain MRI, single-photon emission computed tomography (SPECT), and ^{18}F-fluorodeoxyglucose-PET examinations in each patient. Healthy subject subjects (age range, 20–40 years) without other disorders, including neurological or psychiatric disorders, and who were not taking any drugs were recruited through a notice on the bulletin board of the Biomedical Research Institute of the Seoul National University Hospital. Before inclusion, all subjects underwent a screening interview, neurological and general medical examinations, complete blood count, and

routine biochemical (liver and kidney function) testing. This study was approved by the Institutional Review Board at Seoul National University Hospital and was performed in accordance with the Investigational New Drug application of the Korea Food and Drug Administration (KFDA) and registered at ClinicalTrial.gov (number: NCT02144792).

2. PET/MRI and Experimental Procedures

The PET imaging procedures in our study were performed as described previously.[8] Participants underwent a 60-min PET scan after an intravenous injection of 370 MBq of (*R*)-[^{11}C]-verapamil radiotracer (range, 333-407 MBq). Simultaneous acquisitions of three-dimensional dynamic PET images and T1-weighted MR images were conducted using a Biograph mMR (Siemens, Washington, DC, USA). During the scans, subjects were instructed to lie in a supine position with their heads affixed to a device designed to minimize movement. After routine corrections such as normalization, UTE MRI-based attenuation, scatter, and decay corrections, the PET imaging data acquired in list mode were reconstructed using a filtered back projection. The dynamic volumetric images were sequenced using the following framing: 8 × 2.5 s, 16 × 5 s, 10 × 60 s, and 10 × 240 s. To evaluate Pgp expression, intravenous CS infusion (2.5mg/kg/h and 50mg/mL; Sandimmune; Novartis Pharmaceuticals, Basel, Switzerland) was initiated 1 h before the acquisition of the PET/MRI scans. CS infusion was continued during the PET scan to a maximum of 2 h from the start of the infusion. Blood samples were taken

before and after the PET scan to determine CS concentrations by high-performance liquid chromatography.

To compare the data of (*R*)-[^{11}C]-verapamil PET/MR between tariquidar, a third-generation Pgp inhibitor with enhanced specificity and potency, and CS, one healthy subject underwent a PET/MR scan with both agents. This was performed 3 weeks later as was done in a previous study,[9] under intravenous tariquidar infusion (2mg/kg; Avaant Pharmaceuticals, Woburn, USA).

3. Synthesis of (*R*)-[^{11}C]-verapamil

(*R*)-[^{11}C]-verapamil was synthesized using the previously reported method, with a few modifications.[13] Briefly, [^{11}C]MeI was produced from [^{11}C]CH4 by gas-phase method using a ^{11}C synthesis module (TRACERlab FXC Pro) and then, [^{11}C]MeI was converted into [^{11}C]MeOTf in the AgOTf column. (*R*)-norverapamil (1 mg, 2.27 μmol) was dissolved in MeCN (100 μL), and the precursor solution was injected in the high pressure liquid chromatography (HPLC) loop. And then [^{11}C]MeOTf was released from the module and entered into the loop. The reaction mixture was kept at room temperature for 3 min, and the reaction mixture was purified by preparative HPLC system (the column: YMC Triart C18 10 x 250 mm, S-5 μm; the eluent :10 mM NaOAc:EtOH). From the result of preparative HPLC, two major radioisotope peaks were observed. First peak was expected to be dimethylated product, which would not penetrate the BBB (Figure 1). Second

peak was proven to be (R)-[11C]-verapamil by the retention time comparison with the cold-standard ((*R*)-verapamil) in analytical HPLC chromatogram (Figure 2).

The radiolabelling yield was 13.80 ± 3.13 % (n=20), and the radioactivity of the purified (*R*)-[^{11}C]-verapamil was 3.18±0.80 GBq (n=20) without the decay correction. The specific activity was 243.46±138.01 GBq/μmol (n=20), and the total synthesis time was 15 min ± 2 min (n=20).

4. PET Data Analysis and Acquisition of Asymmetry Indices

PET images were co-registered to the subject's T1-MR images and spatially normalized to a T1 template provided by SPM using SPM8 (Statistical Parametric Mapping) software (Figure 3). Voxel-wise calculations of SUV [voxel intensity [Bq/mL]/(injected dose [Bq]/body weight [g])] was performed in each dynamic PET frame. Dynamic SUVs in 98 brain regions of interest (ROIs) were obtained using the population-based SPAM, which was constructed by incorporating anatomical and functional variabilities among 152 healthy volunteers and automatically labelling brain structures in functional data in MNI space.[14, 15] Because the uptake of (*R*)-[^{11}C]-verapamil in the choroid plexus results in a spill-over of radioactivity into the neighboring medial temporal structures, including the hippocampus, parahippocampal gyrus, and amygdala, we masked out the choroid plexus in the individual normalized PET image, and volumes for hippocampus of the

individually modified SPAM maps were calculated (Table 1). Static SUVs were then obtained as the weighted mean of the dynamic SUVs (Static SUV=$(\frac{Duration\ (ti)}{Total\ time} * SUV(ti)) + \cdots + (\frac{Duration\ (tn)}{total\ time} * SUV(tn)))$ during the 2.5–40 min scans with the frame duration as weight. Based on the static SUVs in each cortex, AIs were calculated using the equation ((right region – left region)/(right region +left region) × 200%) for all the respective participants. If Pgp is overexpressed in the right region, the SUV of (*R*)-[^{11}C]-verapamil in the right region is smaller than that in the left region, resulting in a negative AI. If Pgp is overexpressed in the left region, the SUV in the left region is smaller than that in the right region, resulting in a positive AI. We compared asymmetry in healthy subjects and epilepsy patients using the AIs. To compare the AIs between patients with lateral temporal lobe epilepsy (TLE) and medial TLE group, AIs were assessed in 6 ROI pairs of the temporal lobe. The medial temporal structures included the hippocampus, amygdala, and parahippocampal gyrus. The lateral temporal structures included the superior, middle, and inferior temporal lobes (Figure 4).

5. Genotyping Methods

To investigate whether single-nucleotide polymorphisms (SNPs) related to the expression of Pgp affects the uptake of (*R*)-[^{11}C] verapamil into the brain, we used the genotyping method described by Kim et al.[16] In brief, Genomic DNA was extracted from the peripheral whole blood of each subject using a QIAamp DNA Blood Mini Kit (QIAGEN GmbH, Germany).

Genotyping used TaqMan allelic discrimination assays on an AB 7500 Real time PCR System (Applied Biosystems, Foster City, CA, USA). Genotyping for *ABCB1* 2677G>T, 1236C>T, and 3435C>T single nucleotide polymorphisms (SNPs) were performed using Validated TaqMan Genotyping Assays purchased from Applied Biosystems. PCR reactions were carried out as follows: initial denaturation at 95 ◦C for 10 min, 50 cycles of denaturation at 92 ◦C for 15 s, and then anneal/extension at 60 ◦C for 1 min. The allelic discrimination results were determined after amplification by performing an end-point read. The AB Sequence Detection System 7500 v 1.4 software package (Applied Biosystems) was used in the analyses.

6. Statistical Analyses

Statistical analyses were performed using SPSS for Windows (version 21.0; SPSS Inc., Armonk, NY, USA). A Mann–Whitney *U* test and Fisher's exact test were used to compare the basal characteristics between the DRE and DSE groups, including age, sex, duration of epilepsy, and the number of AEDs taken. In addition, AIs of healthy subjects, DRE patients, and DSE patients were compared using a Mann-Whitney *U* test. Associations between ABCB1 polymorphisms and whole-brain SUVs, and associations between serum concentration of CS and whole-brain SUVs were determined using Spearman's correlation. p-value < 0.05 was considered significant.

RESULTS

1. Basal demographics

Ten healthy men (median age, 27 years [range, 22–36 years]), Ten patients with DRE (median age, 34 years [range, 24–52 years]), and five patients with DSE (median age, 25 years [range 18–53 years]) underwent a VPM-PET/MR–CS. Data from two healthy subjects and two patients were excluded due to technical errors (Figure 5). In two healthy subjects and one DRE patients, the PET/MR stopped working during the scan. One DSE patient did not take the full dose of cyclosporine due to a stop in the infusion pump during the PET/MR scan. Table 2 showed Clinical EEG and brain imaging of patients with drug-resistant and drug- sensitive epilepsy. In the DRE group, patient No.6 had nonlesional frontal lobe epilepsy (FLE) and had a previous history with lesionectomy of the epileptogenic zone in parieto-occipital areas. Patient No.1 had cerebromalacia in the occipital area, however the seizure focus was at the lateral temporal lobe in VEM. Patient No.2 had the longest duration of epilepsy and had lesional lateral TLE with temporal atrophic change. Patient No.3 had nonlesional lateral TLE, and patient No.4 and No.5 had lesional medial TLE with hippocampal sclerosis. Regarding drug-resistant parietal lobe epilepsy (PLE), patient No.7 and No.8 had nonlesional epilepsy, and patient No.9 had a small tuber in the high parietal cortex. In the DSE group, patient No.10 TLE with hippocampal sclerosis,

patient No.11 and No. 12 had nonlesional lateral TLE and patient No.13 had nonlesional FLE.

No difference in basal characteristics was found between the DRE and DSE patients, except for the duration of epilepsy (DRE, median 16 years [range, 5–42 years]; DSE, median 3 years [range, 1–4 years]; p = 0.001), number of AEDs (DRE, median 4 [range 2–4]; DSE, median 1 [range 1–3]; p = 0.019), and seizure frequency (DRE, median 5 per month [range 0.2–30 per month]; DSE, no seizure event per month; p = 0.001) (Table 2).

2. Characteristics of VPM-PET/MR–CS

There was inter-individual variability in the radioactivity of the whole brain in normal participants, and regional distributions of radioactivity were different in each individual (Figure 6A). Moreover, radioactivity of whole brain was independent of the serum concentration of CS (r = 0.100, p = 0.701) and *ABCB1* up-regulation (Figure 6B, Table 3).

In one patient with DSE, CS infusion was discontinued due to a technical problem when the PET/MR scan was initiated. We identified the problem later after termination of the PET/MR scan, leaving the patient to receive CS injection only for an hour before the PET/MR scan. We compared this data with the healthy subjects that were given the CS infusion normally, and found that the radioactivity in the whole brain decreased very rapidly in this patient (Figure 7A).

Five healthy subjects complained of hot flushes in the body during

the infusion of CS, and one healthy subject complained of mild nausea. However, no other side effects were observed during the experimental period.

3. Comparing uptake of (*R*)-[^{11}C] - verapamil between two kinds of Pgp inhibitors

We compared the data of (*R*)-[^{11}C]-verapamil between two kinds of Pgp inhibitors, CS and tariquidar, a third-generation Pgp inhibitor, in one healthy subject. This subject underwent a PET scan with CS, and a PET scan with tariquidar 3 weeks later. There was no difference in the static SUVs between the two Pgp inhibitors (Figure 7B).

4. Different Values of AIs in DRE Patients and Healthy Subjects

All DRE patients, except for patients who had parietal lobe epilepsy, had more asymmetry between ipsilateral ROIs and contralateral ROIs than healthy subjects, while there were no significant differences in AIs between DSE patients and healthy subjects (Figure 7, 9). In TLE, PET data from three patients, two with nonlesional left temporal lobe DRE and one with lesional left temporal lobe DRE, showed significantly more positive AIs than those from healthy subjects (healthy subjects, 4.0413 ± 1.7452; patients, 7.2184 ± 1.8237; p = 0.048), suggesting Pgp overexpression was in the left temporal area. PET data from two patients who had right temporal lobe DRE with

hippocampal sclerosis showed significantly more negative AIs than those from healthy subjects (patients, -1.6496 ± 3.4136; $p = 0.044$), suggesting Pgp overexpression in the right temporal area (Figure 7B).

PET data from a patient who had a right nonlesional frontal lobe DRE showed the largest negative AI. This means that the SUV of the right frontal lobe in this patient was much lower than that of the left frontal lobe, and that the AI of this patient was different from AIs of healthy subjects (healthy subjects, -1.9963 ± 1.6329; patient, -9.0502) (Figure 7A). There was no different AIs between patients with right parietal lobe DRE and healthy subjects (healthy subjects, 2.9557 ± 1.8129; patients, 3.1613 ± 1.4287; $p = 0.921$) (Figure 7C).

In addition, we compared AIs in the temporal lobe between patients with drug-resistant and drug-sensitive left TLE. AIs in patients with DRE were larger than those in patients with DSE, although this result was not statistically significant (DRE, 7.2183 ± 1.8237; DSE, 3.9473 ± 0.5101, $p = 0.100$).

5. Possibility of localization using VPM-PET/MR–CS

We investigated whether localization of the epileptic focus is possible using our method. We compared the characteristics of AIs between the medial TLE and lateral TLE groups. The lateral TLE group had significantly different AIs from those of healthy subjects in the superior (healthy subjects, 3.7592 ± 2.7825; patients, 15.0673 ± 10.2462; p=0.024) and middle temporal gyrus

(healthy subjects, 0.4077 ± 3.0872; patients, 7.3093 ± 1.9225; p = 0.012), but not in the medial temporal structures. Moreover, significant differences in AIs were observed between patients with medial TLE and healthy subjects in the hippocampus but not in the lateral structures (healthy subjects, 10.4622 ± 4.9800; patients, - 4.2948 ± 2.7194; p = 0.044) (Table 4).

DISCUSSION

The primary objective of this study was to confirm the usefulness of non-invasive quantitative PET methods including SPAM with AIs of the SUVs as a surrogate marker in DRE. We also wanted to determine whether this method could help us to localize the epileptic zone. In our study, significant asymmetry of Pgp expression was confirmed in DRE patients with FLE and TLE compared with healthy subjects, and the absolute values of AIs in patients with drug-resistant left TLE also were larger than those in healthy subjects and patients with drug-sensitive left TLE. There was no difference between the DSE group and healthy subjects. In addition, we were able to find different asymmetry patterns between patients with lateral TLE and those with medial TLE.

Two previous studies examined patients with DRE using (*R*)-[^{11}C]-verapamil PET. In a pilot study, (*R*)-[^{11}C]-verapamil PET was performed in seven patients with drug-resistant TLE who had hippocampal atrophy.[17] In this study, the increased efflux (k_2) of (*R*)-[^{11}C]-verapamil in the ipsilateral region was more pronounced than in the contralateral region, although this difference was not statistically significant. In a recent case–control study, 14 patients with drug-resistant TLE caused by unilateral hippocampal sclerosis underwent (*R*)-[^{11}C]-verapamil PET with tariquidar; when compared with DSE patients, the influx (K_1) of (*R*)-[^{11}C]-verapamil was less significantly increased in the patients with drug-resistant TLE.[18] In our study, AIs of the left

TLE group were more positive than those in healthy subjects, suggesting an overexpression of Pgp in the left temporal lobe and a low uptake of (*R*)-[^{11}C]-verapamil. The AIs of the right TLE were also more negative than healthy subjects. In addition, asymmetries in patients with drug-resistant left TLE were larger than those in patients with drug-sensitive left TLE. Considering the coherence of the results of several studies, including our results, (*R*)-[^{11}C]-verapamil PET might serve as an important and useful non-invasive surrogate marker for DRE.

To our knowledge, this is the first report to confirm that (*R*)-[^{11}C]-verapamil PET could facilitate evaluation of a surrogate marker in patients with DRE including neocortical epilepsy. In addition to lateral temporal lobe epilepsy, a patient who had drug-resistant MR-negative right frontal lobe epilepsy had different asymmetry in the frontal lobe to those of healthy subjects. This patient had a much larger negative AI than the healthy subjects, suggesting an overexpression of Pgp in the right frontal lobe. There also was no difference in drug-sensitive frontal lobe epilepsy. Though we examined three patients with PLE, no significant findings were observed in the parietal lobe. In our previous study that was performed using SPAM, there were issues with the SPAM method when the ROI was too large.[19] Small deficits in the high parietal lobule could have been masked due to an averaging effect caused by the normal counts in the posterior section. Also, there were large different AIs among healthy subjects in the parietal lobe. Therefore, larger sample size should be necessary.

For localization, we tried to compare the asymmetry patterns between DRE patients with medial TLE and lateral TLE. All patients with lateral TLE had a significant asymmetry in the superior and middle temporal gyrus, but not in the medial temporal structures. Moreover, two patients with medial TLE had significant different asymmetry in the hippocampus, but not in the lateral temporal structures. Considering the different patterns between the medial and lateral TLE groups, this method could be helpful in localizing the epileptic zone.

Among the cases, a second patient (No. 2) had the longest standing drug-resistant left TLE, and decreased SUV in all of the left lobes indicated broad Pgp overexpression in the left hemisphere. Considering that the DRE group, including this patient, had a longer duration of disease than the DSE group, seizure duration might be an important factor in the overexpression of Pgp. We also analysed the relationship between the duration of epilepsy and the absolute value of the AIs in patients with left DRE and DSE TLE (n=6) using Spearman's non-parametric correlation coefficient, and found a significant correlation (r = 0.928, p = 0.008). Indeed, a recent study investigated the correlation between Pgp overexpression and clinical features (age, age at the onset of habitual seizures, duration of seizure history, seizure frequency per year, and number of Pgp inducers or substrates taken). There was a positive correlation between seizure frequency, number of medications that induce Pgp, and overexpression of Pgp, with no other significant relationships observed.[7] Considering the various results from many studies,

there is ongoing debate regarding which clinical features affect the overexpression of Pgp, and additional studies are required to address this issue.

The use of (*R*)-[^{11}C]-verapamil PET with Pgp inhibitor in humans presents several difficulties. First, high dosages of Pgp inhibitors are unable to be used (*R*)-[^{11}C]-verapamil PET could be used with a medium dosage of a Pgp inhibitor to increase the baseline signal, and thus create larger differences in the brain concentrations of the tracer between the healthy and diseased brains.[9] At an acceptable dose, 17–58% of Pgp inhibition with tariquidar (2–8 mg/kg) and 38–50% of Pgp inhibition with CS (2.5mg/kg/h) were observed by evaluating Pgp inhibition upon (*R*)-[^{11}C]-verapamil PET imaging.[20] Our study produced similar result as the injection of 2mg/kg of tariquidar yielded a slightly lower efficacy compared with CS. However, inter-individual variability regarding affinity and response to the substrate or inhibitor may also complicate the outcome when using a moderate dose of a Pgp inhibitor.[21] Our data also showed individual variability among all the participants, similar to what was observed in previous studies.[10] In addition, the inter-individual variability was unrelated to polymorphisms of the *ABCB1* gene, including *3435T/T* carriers, which had influenced the influx rate of Pgp substrate drug in a previous study.[22] Given the small sample size in our study, we could not determine the influence of these polymorphisms on regional Pgp activity statistically. Second, several studies have shown that the effect of Pgp inhibitors is rapid, and the Pgp function is promptly restored upon the elimination of the inhibitors.[23, 24] Our study showed a rapid decrease in the

radioactivity of the whole brain soon after the infusion of Pgp inhibitor was terminated, despite the maintenance of the serum concentration of CS. Therefore, a novel Pgp inhibitor with enhanced affinity and a longer half-life for binding Pgp will be required.

This study has several limitations. First, due to the small sample size in each group, we were unable to detect statistically significant differences in patients with frontal epilepsy. However, despite the small sample size, we showed robust differences in the asymmetry patterns of patients with DRE from healthy subjects and patients with DSE. Second, our study did not consider cerebral blood flow measurements. The regional uptake of (R)-[11C]-verapamil can become dependent on regional cerebral blood flow when Ppg is partially inhibited.[25] However, because (*R*)-[^{11}C]-verapamil is a low-extraction radiotracer, the uptake of (*R*)-[^{11}C]-verapamil is considered to be insensitive to changes in cerebral blood flow.[10] In addition, Muzi et al. reported that the CS modulation of Pgp increased the blood-brain transfer of (*R*)-[^{11}C]-verapamil into the brain by 73%, and this increase was significantly greater than changes in blood flow by 13%.[8]

Despite some problems with the use of VPM-PET/MR-CS, considering the different asymmetry in the DRE group, but not in the DSE group, from that of healthy subjects, the AI could be a useful surrogate marker of DRE in clinical practice. In addition, DRE patients exhibiting Pgp overexpression could be treated with a Pgp inhibitor. A recent pilot study reported that the adjunctive use of verapamil (120 mg/day), which was used

as a Pgp inhibitor in DRE patients, improved the response rate.[26] In the future, our method should be applied to more variable neocortical epilepsy cases.

CONCLUSION

Based on the results obtained to date, we confirmed the importance of Pgp expression in DRE using a non-invasive method including SPAM analysis with AIs. Therefore, an AI obtained using VPM-PET/MR-CS might be used as a surrogate marker of Pgp expression in patients with epilepsy, and might serve as an important prognostic factor for individualized drug therapy. Moreover, the results showing that ipsilateral lesions had low SUVs, and the difference in asymmetry patterns between medial and lateral temporal epilepsy groups showed that our method may be a useful tool for localization of the epileptic zone. In the future, prospective studies using VPM-PET/MR-CS in patients with recent-onset epilepsy are necessary for assessing predictive value.

REFERENCES

1. Browne TR, Holmes GL. Epilepsy. *N Engl J Med* 2001;344:1145-1151

2. Loscher W, Schmidt D. Modern antiepileptic drug development has failed to deliver: ways out of the current dilemma. *Epilepsia* 2011;52:657-678

3. Sillanpaa M, Schmidt D. Natural history of treated childhood-onset epilepsy: prospective, long-term population-based study. *Brain* 2006;129:617-624

4. Loscher W, Klitgaard H, Twyman RE, et al. New avenues for anti-epileptic drug discovery and development. *Nat Rev Drug Discov* 2013;12:757-776

5. Loscher W, Potschka H. Drug resistance in brain diseases and the role of drug efflux transporters. *Nat Rev Neurosci* 2005;6:591-602

6. Potschka H. Role of CNS efflux drug transporters in antiepileptic drug delivery: overcoming CNS efflux drug transport. *Adv Drug Deliv Rev* 2012;64:943-952

7. Liu JY, Thom M, Catarino CB, et al. Neuropathology of the blood-brain barrier and pharmaco-resistance in human epilepsy. *Brain* 2012;135:3115-3133

8. Muzi M, Mankoff DA, Link JM, et al. Imaging of cyclosporine inhibition of P-glycoprotein activity using 11C-verapamil in the brain: studies of healthy humans. *J Nucl Med* 2009;50:1267-1275

9. Wagner CC, Bauer M, Karch R, et al. A pilot study to assess the

efficacy of tariquidar to inhibit P-glycoprotein at the human blood-brain barrier with (R)-11C-verapamil and PET. *J Nucl Med* 2009;50:1954-1961

10. Bauer M, Karch R, Neumann F, et al. Assessment of regional differences in tariquidar-induced P-glycoprotein modulation at the human blood-brain barrier. *J Cereb Blood Flow Metab* 2010;30:510-515

11. Dukart J, Mueller K, Horstmann A, et al. Differential effects of global and cerebellar normalization on detection and differentiation of dementia in FDG-PET studies. *NeuroImage* 2010;49:1490-1495

12. Kwan P, Arzimanoglou A, Berg AT, et al. Definition of drug resistant epilepsy: consensus proposal by the ad hoc Task Force of the ILAE Commission on Therapeutic Strategies. *Epilepsia* 2010;51:1069-1077

13. Luurtsema G, Windhorst AD, Mooijer MP, et al. Fully automated high yield synthesis of (R)-and (S)-[11C] verapamil for measuring P-glycoprotein function with positron emission tomography. *J Labelled Comp Radiopharm* 2002;45:1199-1207

14. Kang KW, Lee DS, Cho JH, et al. Quantification of F-18 FDG PET images in temporal lobe epilepsy patients using probabilistic brain atlas. *NeuroImage* 2001;14:1-6

15. Lee JS, Lee DS. Analysis of functional brain images using population-based probabilistic atlas. *Current Medical Imaging Reviews* 2005;1:81-87

16. Kim DW, Lee SK, Chu K, et al. Lack of association between ABCB1, ABCG2, and ABCC2 genetic polymorphisms and multidrug resistance in

partial epilepsy. *Epilepsy Res* 2009;84:86-90

17. Langer O, Bauer M, Hammers A, et al. Pharmacoresistance in epilepsy: a pilot PET study with the P-glycoprotein substrate R-[(11)C]verapamil. *Epilepsia* 2007;48:1774-1784

18. Feldmann M, Asselin MC, Liu J, et al. P-glycoprotein expression and function in patients with temporal lobe epilepsy: a case-control study. *Lancet Neurol* 2013;12:777-785

19. Lee SK, Lee DS, Yeo JS, et al. FDG-PET images quantified by probabilistic atlas of brain and surgical prognosis of temporal lobe epilepsy. *Epilepsia* 2002;43:1032-1038

20. Kalvass JC, Polli JW, Bourdet DL, et al. Why clinical modulation of efflux transport at the human blood-brain barrier is unlikely: the ITC evidence-based position. *Clin Pharmacol Ther* 2013;94:80-94

21. Syvanen S, Eriksson J. Advances in PET imaging of P-glycoprotein function at the blood-brain barrier. *ACS Chem Neurosci* 2013;4:225-237

22. Taubert D, von Beckerath N, Grimberg G, et al. Impact of P-glycoprotein on clopidogrel absorption. *Clin Pharmacol Ther* 2006;80:486-501

23. Syvanen S, Blomquist G, Sprycha M, et al. Duration and degree of cyclosporin induced P-glycoprotein inhibition in the rat blood-brain barrier can be studied with PET. *NeuroImage* 2006;32:1134-1141

24. Syvanen S, Hooker A, Rahman O, et al. Pharmacokinetics of P-glycoprotein inhibition in the rat blood-brain barrier. *J Pharm Sci*

2008;97:5386-5400

25. Deo AK, Borson S, Link JM, et al. Activity of P-Glycoprotein, a beta-Amyloid Transporter at the Blood-Brain Barrier, Is Compromised in Patients with Mild Alzheimer Disease. *J Nucl Med* 2014;55:1106-1111

26. Asadi-Pooya AA, Razavizadegan SM, Abdi-Ardekani A, et al. Adjunctive use of verapamil in patients with refractory temporal lobe epilepsy: a pilot study. *Epilepsy Bebav* 2013;29:150-154

TABLES

Table 1. Volume of hippocampal regions in healthy subjects and patients with temporal lobe epilepsy

Subjects	L_Hippocampus (mm^3)	R_hippocampus (mm^3)
Healthy subjects		
Subject 1	**13520**	**10504**
Subject 2	**12928**	**9664**
Subject 3	**12832**	**9880**
Subject 4	**13296**	**10448**
Subject 5	**13160**	**10440**
Subject 6	**13808**	**10720**
Subject 7	**12928**	**9664**
Subject 8	**13848**	**10616**
Patients with temporal lobe epilepsy		
1	**11872**	**9008**
2	**11896**	**9120**
3	**13360**	**9920**
4	**12184**	**9400**
5	**13408**	**10464**
11	**12768**	**10152**
12	**13160**	**10040**
13	**13656**	**10896**

Table 2. Clinical EEG and brain imaging of patients with drug-resistant and drug- sensitive epilepsy.

Patient Number	Sex, age	Syndrome	Duration of epilepsy	Average seizure frequency (month)	Antiepileptic drugs	Video EEG monitoring	Brain MRI	Ictal SPECT	Interictal SPECT	FDG-PET
Drug-resistant epilepsy										
1	M,44	TLE	34	1	CBZ, TPM, VPA, PB	Lt. lateral TLE	Cerebromalatic changes at the right cuneus and left lingual gyrus	N/A	N/A	Normal
2	F, 52	TLE	42	2	CBZ, VPA, LEV	Lt. lateral TLE	Atrophic change, left temporal lobe	N/A	N/A	N/A
3	F,29	TLE	5	0.5	LEV, OXC, LMT	Lt. lateral TLE	Normal	N/A	N/A	Hypometabolism in left temporal lobe
4	M,43	TLE	37	30	CBZ, VPA, LEV, TPM	Rt. medial TLE	Hippocampal sclerosis, Rt.	N/A	N/A	Hypometabolism in right temporal lobe

5	F,29	TLE	12	0.2	LEV, CBZ	Rt. medial TLE	Hippocampal sclerosis, Rt.	N/A	N/A	Hypometabolism in right medial temporal lobe
6	F,26	FLE	15	30	VPA, CBZ, TPM, PB	Rt. FLE	Lesionectomy in the right high parietal cortex	Hyper perfusion in the right posterior–inferior frontal lobe	N/A	N/A
7	F,34	PLE	16	8	PHT, LEV, CBZ, TPM	Not localization, suspicious Rt. PLE*	Normal	Hyperperfusion in the right parietal lobe and left frontal lobe	Normal	Normal
8	F,24	PLE	10	5	OXC, ZNS	Not localization, suspicious Rt. PLE*	Normal	N/A	N/A	N/A
9	M,34	PLE	16	30	PHT, LEV	Not localization, suspicious Rt. PLE*	Small tuber in Rt. high parietal cortex	N/A	N/A	N/A

Drug-sensitive epilepsy										
10	M, 21	TLE	4	0	VPA, ZNS, LEV	Lt.medial TLE	Hippocampal sclerosis	N/A	N/A	N/A
11	M, 18	TLE	4	0	LEV, OXC	Lt.lateral TLE	Normal	N/A	N/A	N/A
12	M, 18	TLE	1	0	LEV	Lt.lateral TLE	Normal	N/A	N/A	N/A
13	M, 18	FLE	1	0	LEV	Lt.FLE	Normal	N/A	N/A	N/A

FLE, frontal lobe epilepsy; TLE, temporal lobe epilepsy; LEV, levetiracetam; OXC, oxcarbazepine; VPA, valproic acid; ZNS, zonisamide; CBZ, carbamazepine; TPM, topiramate; PB, phenobarbital; PHT, phenytoin; LMT, lamotrigine; N/A, not applicable. * diagnosed by seizure semiology

Table 3. Radioactivity in whole brain (SUV) and *ABCB1* genotype

No.	Radioactivity in whole brain (SUV)	ABCB1(MDR1)		
		1236 C>T rs1128503	2677 G>T,A rs2032582	3435 C>T rs2032582
Healthy subjects				
Subject 1	0.47883	CT	GA	CC
Subject 2	0.53917	CT	GT	CT
Subject 3	0.36889	TT	TT	CT
Subject 4	0.45964	CT	AA	CC
Subject 5	0.52468	CT	GG	CC
Subject 7	0.43680	CT	TA	CT
Drug-resistant epilepsy				
2	0.78392	CT	TA	CT
4	0.62644	CT	GT	CT
6	0.34171	CT	GT	CT
7	0.46389	CT	GT	CT
8	0.62687	CC	GA	CC
9	0.55521	CT	GT	CT
Drug-sensitive epilepsy				
11	0.46978	CT	GG	CC
13	0.41311	TT	GT	CT

Table 4. Comparison of AIs in temporal structures among healthy subjects and patients with drug-sensitive and drug-resistant lateral and medial temporal lobe epilepsy

Variables	Superior temporal gyrus	*P*-value	Middle temporal gyrus	*P*-value	Inferior temporal gyrus	*P*-value	Hippo-Campus	*P*-value	Parahippo-campus	*P*-value	Amygdala	*P*-value
Healthy subjects (mean ± SD)	3.7592± 2.7825		0.4077± 3.0872		6.4996± 5.9187		10.4621 ± 4.9800		3.0562 ± 4.7347		7.3099 ± 10.5752	
Drug-resistant epilepsy												
Lateral temporal lobe		**0.024**		**0.012**		0.133		0.497		0.776		0.776
No.1	**12.0210**		**6.1940**		2.5146		6.6514		2.0533		0.6077	
No. 2	**26.4911**		**9.5291**		-13.9591		6.1304		1.0569		12.0481	
No. 3	**6.6896**		**6.2048**		7.8915		9.3431		5.3695		15.3958	
Medial temporal lobe		0.400		0.178		0.089		**0.044**		0.400		0.267
No. 4	-2.2631		-2.6759		3.0665		**-2.3718**		-1.3807		-5.9779	
No. 5	2.7266		-3.6833		-8.1621		**-6.2177**		2.5178		1.2254	
Drug-sensitive epilepsy												
Lateral temporal lobe		0.400		1.000		0.400		0.889		0.711		0.267
No. 11	5.3757		0.9214		5.9762		1.2332		-2.9354		-5.5809	
No. 12	5.2332		0.9663		-3.4403		14.6596		5.8813		4.7310	
Medial temporal lobe												
No. 10	4.6689		1.2125		1.5589		2.3679		-2.2080		7.7990	

FIGURES

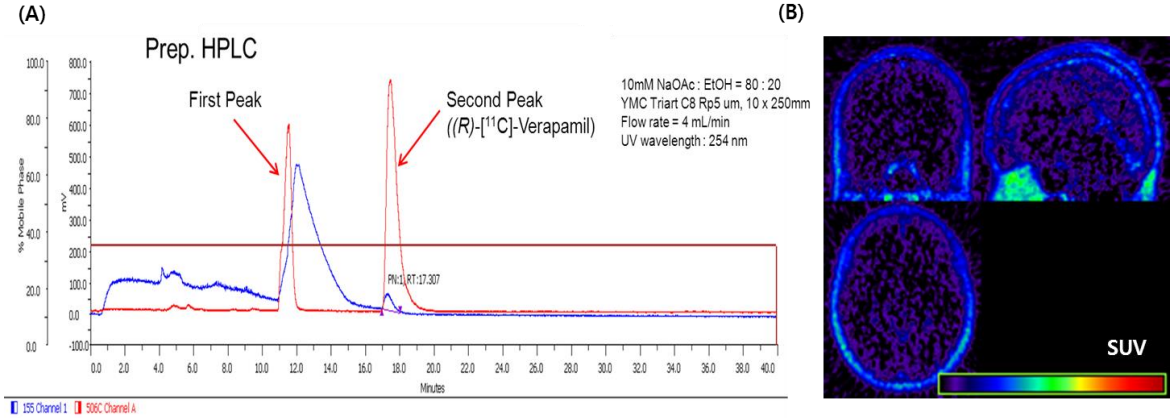

Figure 1. (A) Preparative HPLC chromatogram of (*R*)-[^{11}C]-verapamil synthesis. Two major radioisotope peaks were observed. (B) No radioactivity of whole brain in the PET scans as using the first radioisotope peak.

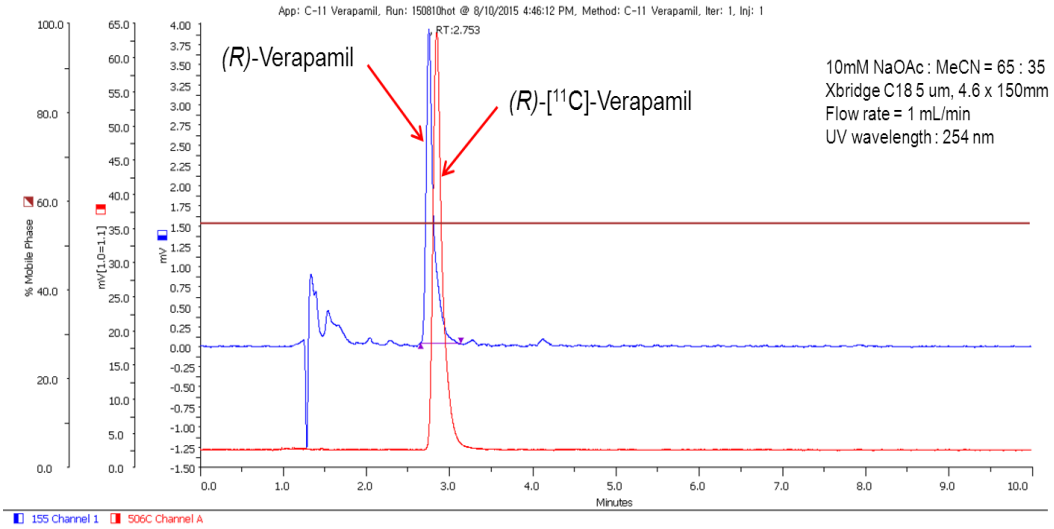

Figure 2. Analytical HPLC chromatogram of (*R*)-[^{11}C]-verapamil and the cold-standard.

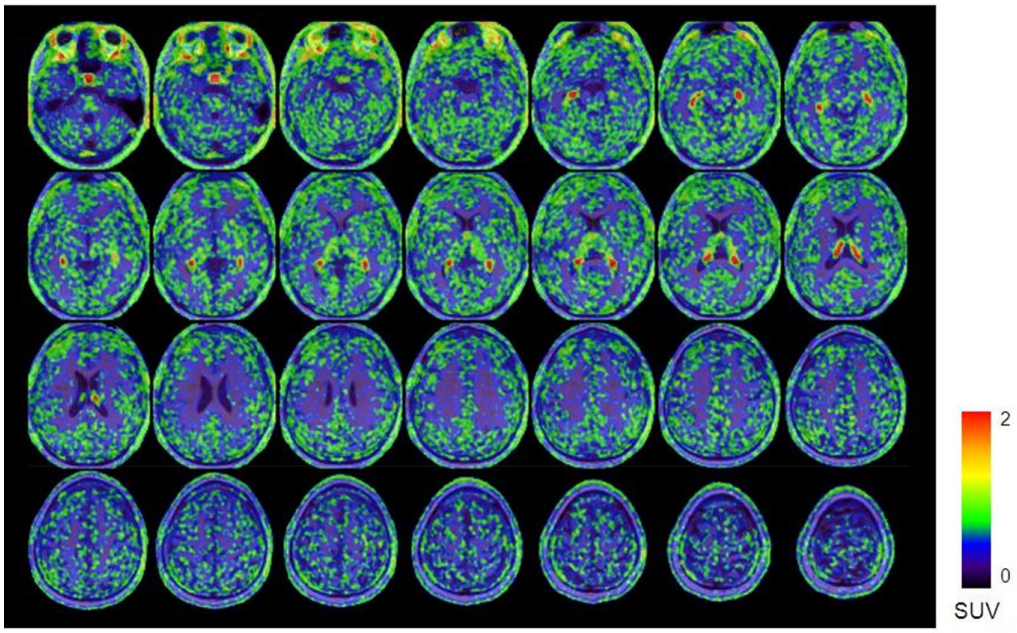

Figure 3. (*R*)- [^{11}C]-Verapamil PET/MR uptake images with cyclosporine infusion in a patient who had drug-resistant left neocortical temporal lobe epilepsy. The colour scale reflects the SUV as shown by the heat map.

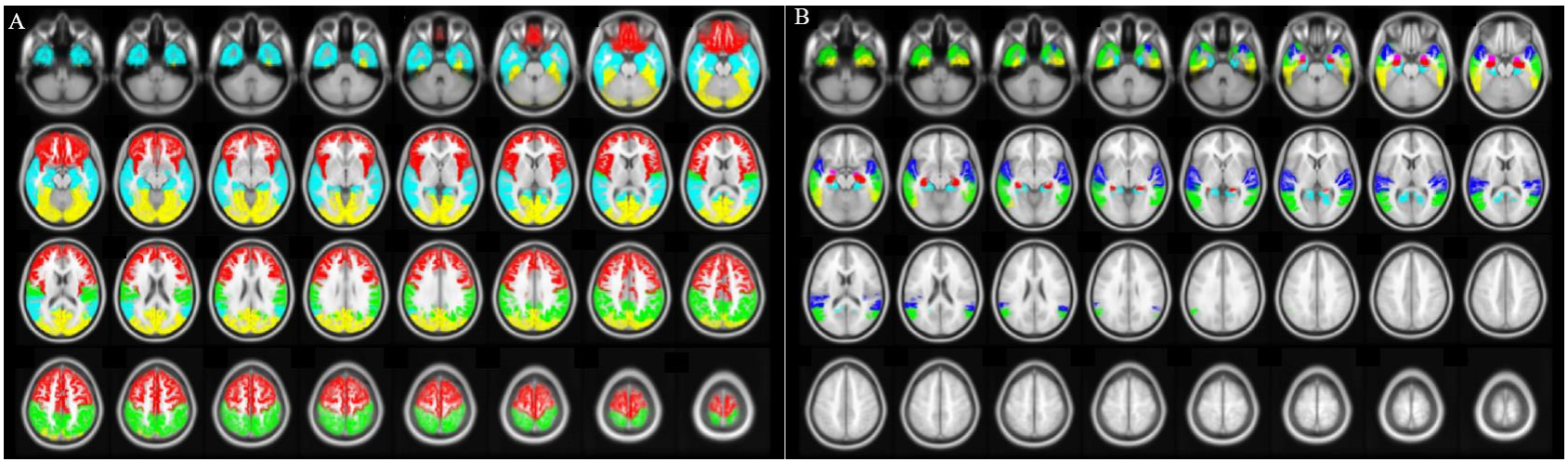

Figure 4. (A) T1-weighted MR images (axial view) marking volumes of interest including the frontal, parietal, temporal, occipital cortices, and (B) temporal regions of interest including the hippocampus, amygdala, parahippocampus, superior temporal gyrus, middle temporal gyrus, inferior temporal gyrus by the population-based SPAM. (A) Red, frontal cortex; cyan, temporal cortex; green, parietal cortex; yellow, occipital cortex. (B) Red, hippocampus; violet, amygdala; cyan, parahippocampus; blue, superior temporal gyrus; green, middle temporal gyrus; yellow, inferior temporal gyrus.

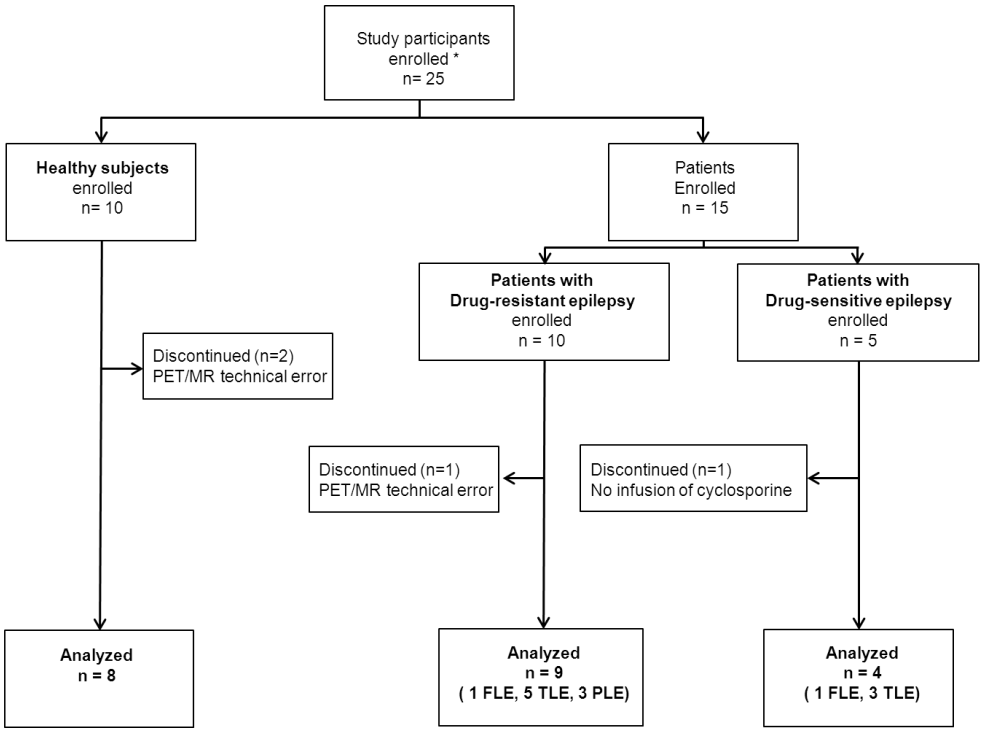

Figure 5. Patient flow

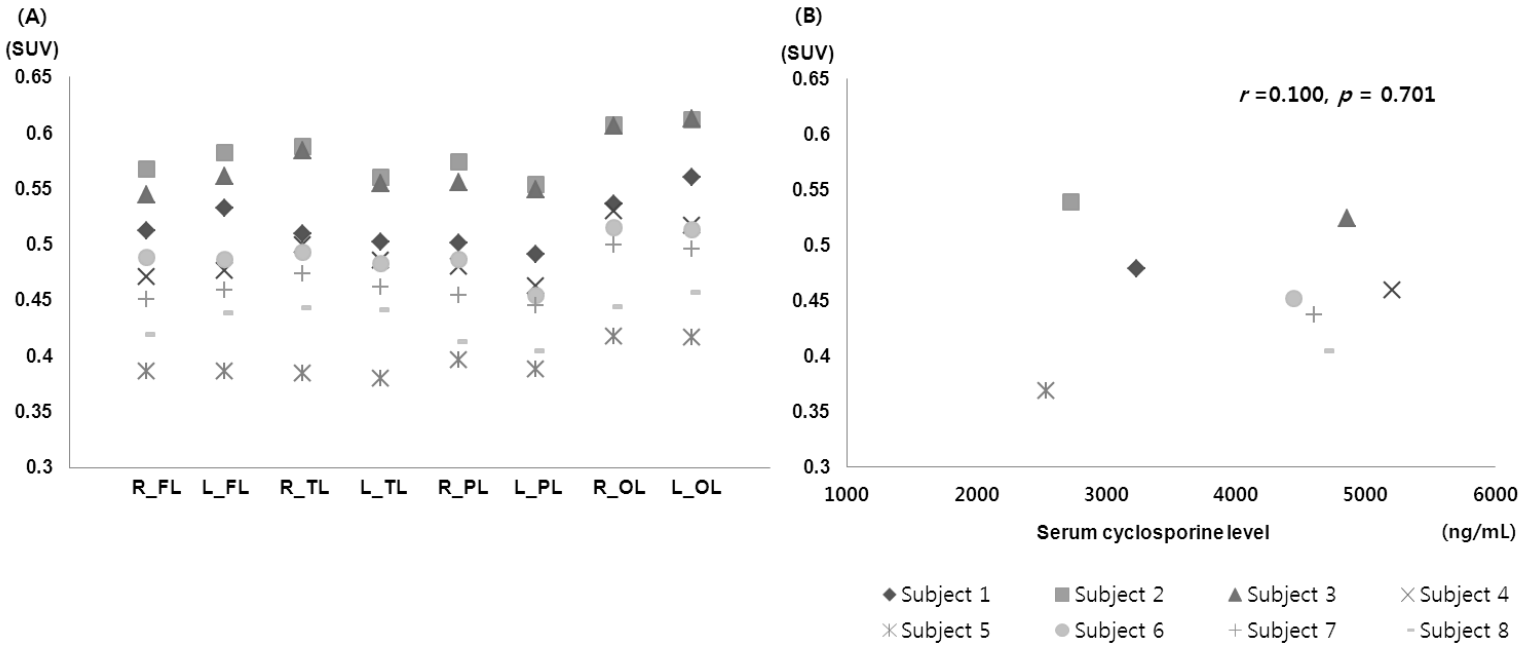

Figure 6. (A) Radioactivity of the whole brain and regional distributions of radio uptakes in healthy subjects. (B) Relationship between the radioactivity of the whole brain in healthy subjects and the serum concentration of CS (r = 0.100, p = 0.701).

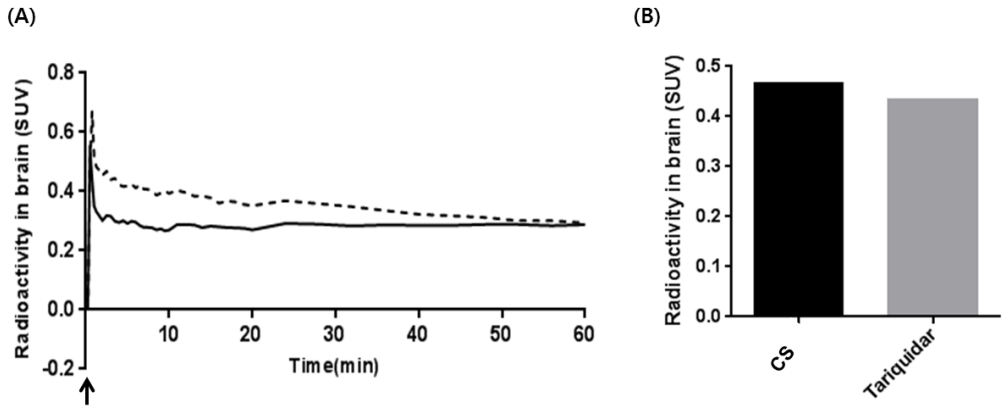

Figure 7. (A)Time-activity curves of (*R*)-[^{11}C]-verapamil in whole-brain from 0 to 60 min for PET scan in a patient (dash line) and a healthy subject (dot line). In PET scan of a patient, infusion of cyclosporine (CS) was discontinued when the PET scan was started. Arrow indicates the discontinuation time of CS. (B) Whole brain static SUV of (*R*)-[^{11}C]-verapamil for PET/MR scan with tariquidar and with CS in a healthy subject.

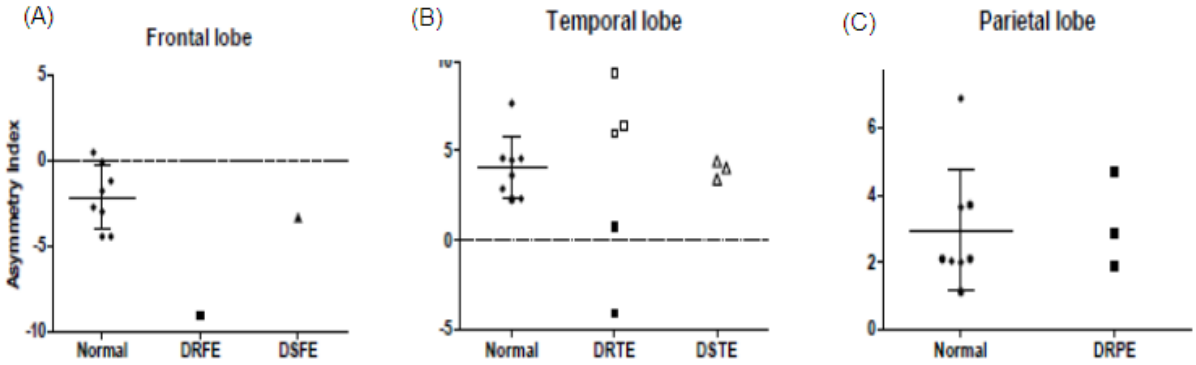

Figure 8. (A) Asymmetry indices (AIs) of the frontal lobes in healthy subjects and in patients with drug-resistant or drug- sensitive right frontal lobe epilepsy. (B) AIs of temporal lobes in healthy subjects and in patients with drug-resistant or –sensitive temporal lobe epilepsy. Filled squares were diagnosed right temporal lobe epilepsy, and blank squares and triangles were diagnosed left temporal lobe epilepsy. (C) AIs of parietal lobe in healthy subjects and in patients with drug–resistant right parietal lobe epilepsy. When the AI was positive, the standard uptake value (SUV) of ^{11}C-Verapamil in the left region was lower than that in the right region in each paired lobe. The bars represent the means ± standard deviations.; DRFE, drug-resistant frontal lobe epilepsy; DSFE, drug-sensitive frontal lobe epilepsy; DRTE, drug-resistant temporal lobe epilepsy; DSTE, drug-sensitive temporal lobe epilepsy.

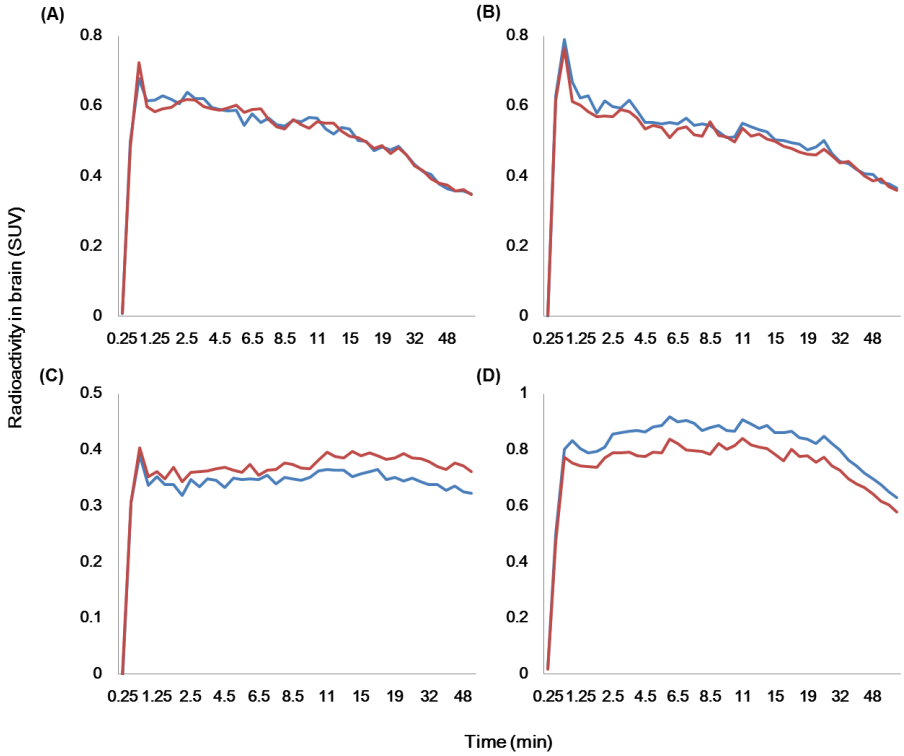

Figure 9. The time-activity curves of (*R*)-[^{11}C]-verapamil in (A) the frontal lobe of a healthy subject; (B) the temporal lobe of a healthy subject; (C) the frontal lobe of Patient No.6, who had drug-resistant right frontal lobe epilepsy; and (D) the temporal lobe of Patient No.2, who had drug-resistant left temporal lobe epilepsy. Blue line, right lobe; red line, left lobe.

국문요약

연구 배경 및 목적: 난치성 뇌전증 환자의 약제 저항성을 설명하는 주 가설 중 하나로 뇌혈관장벽 및 뇌실질의 P-glycoprotein 수용체의 발현에 의한 작용부위의 약물 흡수율의 저하가 잘 알려져 있다. 그러나 뇌에 작용하는 물질의 정량적 측정이 어려워 실제 임상에서 P-glycoprotein의 발현을 정량화 할 수 있는 대리표지자가 없고 임상연구도 활발히 이루어지지 못하고 있다. 이에 우리는 P-glycoprotein 억제제인 사이클로스포린 A와 (R)-[11C]-verapamil PET/MRI을 이용하여 약제 저항성 난치성 뇌전증의 대리표지자를 개발하고자 한다.

연구방법: 본 연구는 P-glycoprotein의 뇌실질 내 발현을 관찰하기 위해 9명의 건강한 성인의 정상군, 5명의 약제 민감성 뇌전증 환자군 그리고 9명의 약제 저항성 뇌전증 환자군에서 P-glycoprotein의 억제제인 사이클로스포린 A를 주사하면서 (R)-[11C]-verapamil 뇌 PET/MRI을 촬영하였다. 뇌의 통계적 확률뇌지도(statistical probabilistic anatomical map, SPAM)를 사용하여 뇌의 98 관심구역 내 (R)-[11C]-verapamil의 표준화섭취계수(Standard uptake value, SUV)를 구한 뒤, 병소를 포함한 영역와 병소 반대편 영역의 SUV를

이용하여 비대칭성 지수 [(우측 영역 – 좌측 영역)/(우측 영역 + 좌측 영역) ×200%]를 계산하였다.

연구결과: 측두엽과 전두엽 영역 내 병소를 가진 모든 약제 저항성 뇌전증 환자들은 정상군과 다른 양상의 비대칭성 지수를 가졌으나, 모든 약제 민감성 환자들은 정상군과 유사한 비대칭성 보여 주었다. 측두엽 영역의 비대칭성 지수 비교 시, 좌측 측두엽을 병소로 가진 약제 저항성 뇌전증 환자들은 정상군에 비해 통계적으로 유의한 더 큰 양의 값을 가졌고(정상군: 4.0413 ± 1.7452; 환자군: 7.2184 ± 1.8237; p = 0.048), 우측 측두엽을 병소로 가진 약제 저항성 뇌전증 환자들은 정상인에 비해 통계적으로 유의한 더 큰 음의 값을 가졌다(patients: -1.6496 ± 3.4136; p = 0.044). 더욱이 측두엽의 영역을 세분화하여 분석 시, 외측 측두엽을 병소로 가진 약제 저항성 뇌전증 환자들은 외측 측두엽 부위에서 정상군과 다른 비대칭성 지수를 가졌으며, 내측 측두엽을 병소로 가진 약제 저항성 뇌전증 환자들은 내측 측두엽 부위에서 정상군과 다른 비대칭성 지수를 가졌다. 전두엽 영역의 비대칭성 지수를 비교 시, 우측 전두엽을 병소로 가진 약제 저항성 뇌전증 환자는 정상군보다 더 큰 음의 값을 가졌다. 두정엽 영역의 비대칭성 지수 비교 시에는 정상군과 약제 저항성 뇌전증 환자군에서 비대칭성 지수의 차이를 보이지 않았다.

결론: 본 연구를 통해 사이클로스포린 A와 (R)-[11C]-verapamil PET/MRI를 이용하여 얻는 비대칭성 지수가 P-glycoprotein 과발현에 의한 약제 저항성 뇌전증의 대리표지자로 유용할 수 있음 입증하였다. 또한 뇌전증 병소를 편측화 및 국소화 하는 세분화 분석도 가능함을 보여주었다.

주요어: P-glycoprotein, 약제 저항성 뇌전증, 대리표지자, PET/MR, (R)-[11C]-Verapamil

학번: 2012-21775